


Article

Preparation of Polyurethane-Modified Silicone Rubber Insulating Coating and Its Application in 10 kV Overhead Bare Wire Wrapping

Wei Wang¹, Fan Yang², Pan Zhang², Zhi Luo², Fangya Li², Jingjing Jiang², Jianbing Zhang², Wei Li^{1,*}, Aimei Liu^{1,*} and Caiqin Qin¹ 

¹ School of Chemistry and Materials Science, Hubei Engineering University, Xiaogan 432000, China; weiwang@hbeu.edu.cn (W.W.)

² State Grid Hubei Electric Power Company Co., Ltd., Xiaogan Power Supply Company, Xiaogan 432000, China

* Correspondence: weili@hbeu.edu.cn (W.L.); liuam@hbeu.edu.cn (A.L.)

Abstract: Room-temperature vulcanized rubber is an excellent polymer material with excellent electrical insulation and mechanical properties, which can be used for field insulation of high-voltage bare wire. In this paper, a room-temperature cured coating material was prepared from α,ω -dihydroxy polydimethylsiloxane (PDMS), polyurethane-modified silicone material (PU-Si), and Methyltris(methylethylketoxime) silane (MOS). The study showed that the coating made by adding PDMS (70 g), PU-Si (30 g), CaCO_3 (90 g), MOS (7 g), KH792 (5 g), and $\text{Mg}(\text{OH})_2$ (30 g) had a surface drying time of 19.1 min, tensile strength of 3.2 Mpa, volume resistivity greater than $4 \times 10^{14} \Omega \cdot \text{cm}$, breakdown voltage greater than 20 kV/mm, and flame retardant performance of the FV-1 level. The comprehensive performance of the insulation material meets the national standard of “Aerial insulated cables for rated voltage of 10 kV” (GB/T14049-2008), while the insulation material has been successfully applied to the overhead line renovation project of the State Grid Hubei Electric Power Company (Wuhan, China).

Keywords: silicone rubber; polyurethane; coatings; cables; bare wire wrapping



Citation: Wang, W.; Yang, F.; Zhang, P.; Luo, Z.; Li, F.; Jiang, J.; Zhang, J.; Li, W.; Liu, A.; Qin, C. Preparation of Polyurethane-Modified Silicone Rubber Insulating Coating and Its Application in 10 kV Overhead Bare Wire Wrapping. *Coatings* **2023**, *13*, 837. <https://doi.org/10.3390/coatings13050837>

Academic Editor: Alicia de Andrés

Received: 28 March 2023

Revised: 21 April 2023

Accepted: 25 April 2023

Published: 26 April 2023



Copyright: © 2023 by the authors. Licensee MDPI, Basel, Switzerland. This article is an open access article distributed under the terms and conditions of the Creative Commons Attribution (CC BY) license (<https://creativecommons.org/licenses/by/4.0/>).

1. Introduction

The widespread distribution and complex structure of overhead conductors [1–3] can easily trip in stormy weather and affect the safety and reliability of the power supply. Insulation of overhead bare wires, which can avoid grid failures due to natural causes, is the best way to ensure the safe and stable operation of the line. Conventional methods of modifying the insulation of bare wires include the replacement of wires and the coating of bare wires. Yet, these methods require arranging relevant line outages, which seriously affects power supply reliability. The use of insulation coating robots [4–6] to conduct the electric insulation spraying of wires can effectively solve the safety hazards of bare wire, not only to protect the reliability of the power supply and provide residential electrical safety, but also to reduce the operational risk of operators.

In 2018, the State Grid Corporation of China decided to strengthen the promotion and application of the new technology of “Spraying insulating paint with electricity”, which led to coated insulation becoming one of the materials used for the insulation wrapping of overhead conductors. Therefore, the development of insulating coatings that can be applied online is of great importance for power transmission [7–9]. In addition to their excellent electrical and insulating properties, the coated insulating materials require good flow and fast drying properties under normal outdoor conditions. Since the 1950s, due to its excellent electrical and mechanical properties, crosslinked polyethylene (XLPE) [10] has replaced thermoplastic polyethylene as the most widely used cable insulation material, but XLPE has poor fluidity and cannot be used directly in extruded insulated high-voltage cables.

The electrical properties of isotactic polypropylene [11] are closer to those of polyethylene, but the melting temperature is higher, and it is also unsuitable for the construction of overhead cables. Room-temperature vulcanized silicone rubber (RTV), easily extruded and molded at room temperature, is the most suitable insulating coating for field application. RTV [12–16] is a silicone elastomer with a basic Si-O-Si backbone. It is vulcanized with water vapor at room temperature to form a material with aging resistance, stain resistance, and high electrical insulation properties. Of particular importance is the fact that its electrical strength does not change over a wide temperature range. Due to its good electrical properties, RTV is often used as an anti-flash material for insulators in power systems. Compared to epoxy [17–19], polyurethane [20–22], and polyethylene polymers [23–26], RTV polymers have poor mechanical properties and poor adhesion to metals. Therefore, it is necessary to combine RTV materials with other organic molecules through copolymerization (blocking and grafting) or blending to improve the performance of RTV polymers and expand the scope of use of RTV materials [27–31]. Polyurethane (PU) [32–34] has strong mechanical properties, wear resistance, and strong adhesion characteristics. The polyurethane embedded in the polymer molecular chain, while maintaining the properties of silicone resistance to high and low temperatures and insulation properties, can improve the adhesion of silicone, wear resistance, chemical resistance, and other properties.

Our group has long been working with the State Grid Xiaogan Power Supply Company (Xiaogan, China) on the purification of transformer insulating oil and the protection and repair of power supply equipment [35–37]. In this paper, a de-ketoxime type room-temperature vulcanized rubber was prepared. By adding a certain amount of polyurethane-modified silicone material to the basic formulation, we studied shortening the surface drying time of RTV and improving the physical and mechanical properties and adhesion of RTV, so that it can meet the demand of 10 kV high-voltage insulating coating. A prepolymer of polyurethane-modified hydroxyl silicone oil (PU-Si) was first synthesized using the bridging effect of isophorone diisocyanate (IPDI), and the optimum synthesis process of the prepolymer was determined by the acetone-di-n-butylamine method [38]. The prepolymer was then blended with α,ω -dihydroxy polymethylsiloxane (PDMS), methyltributylketoxime silane (MOS), silicone coupling agent (KH792), and fillers (SiO_2 and CaCO_3) to obtain the cable cladding material. The structure and properties of the insulating materials were characterized using infrared spectroscopy (FTIR), thermogravimetric analysis (TG), and scanning electron microscopy (SEM), which showed that the introduction of polyurethane functional groups improved the mechanical and adhesive properties of the insulating materials and can meet the requirements for the high performance of the insulating materials.

2. Materials and Methods

2.1. Materials

Dihydroxy polydimethylsiloxane (average $M_n \sim 1500$, viscosity ~ 35 cst), isophorone diisocyanate (AR, $\geq 98\%$), silica ($\geq 99.8\%$, particle size: 7–40 nm), nano calcium carbonate ($\geq 99\%$), dimethyl silicone oil (viscosity: 1000 mPa·s), dibutylamine (AR), $\text{Mg}(\text{OH})_2$ (AR), acetone (AR), hydrochloric acid, and bromocresol green (RG) were purchased from West Asia Chemical Technology (Shandong, Co. Ltd, Jinan, China). Methyltris (methylethylketoxime) silane (KH 301, $\geq 95\%$, MOS), dibutyltin laurate (AR), and N-aminoethyl- γ -aminopropyltrimethoxysilane (KH792, $\geq 95\%$) were purchased from Nanjing Jingtianwei Chemical Co., Ltd. (Nanjing, China).

2.2. Analytical Methods and Test Standards

The coating was made into a film material by a press vulcanizer, and its microstructure and thermal and mechanical properties were tested after complete curing. An electronic universal testing machine (AG-IC 5 KN IS, Shimadzu, Kyoto, Japan) was used to test the mechanical properties of the films. Infrared spectroscopy (FTIR, FTIR-850, Tianjin Gangdong, Tianjin, China) was used to check whether the prepolymer (PU-Si) was successfully

prepared. The thermal stability of the membranes was analyzed with a thermogravimetric analyzer (TG, STA449F5, Netzsch, Selb, Germany), with test conditions set at a heating rate of 10 °C/min at N₂ flow (50 mL/min). Scanning electron microscopy (JEOL, JSM-6510, Tokyo, Japan) was used to test the morphology of the coatings after curing.

The surface drying performance and depth of cure performance indexes were tested under standard laboratory conditions at (25 °C + 2 °C) and (50% + 5%) humidity.

Surface drying time: tested according to standard GB/T 13477.5-2002.

Curing depth: tested according to standard GB/T 32369-2015.

Hardness: tested according to GB/T 2411-2008.

Tensile strength and elongation at break: tested according to GB/T 528-2009; the flat film was taken and cut into 2.50 cm × 0.4 cm samples.

Flame retardant performance: tested according to GB/T10707.2008.

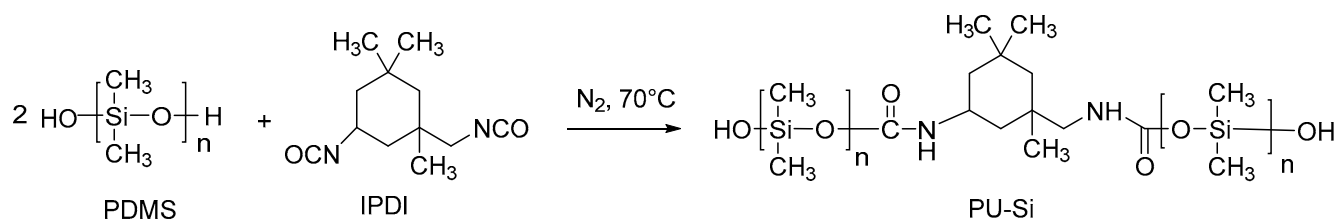
Tensile shear strength: tested according to GB/T-13936-2014.

Electrical breakdown strength: tested according to ASTM D1498.

Volume resistivity: tested according to GB/T1692-2008.

2.3. Synthesis of Prepolymer (PU-Si)

The synthesis method was followed as in reference [39]. Briefly, in a 100 mL flask with a stirring, condensing, and temperature control device, 10 g of IPDI was added, stirred at 500 r/min, ventilated with nitrogen, and heated to 70 °C. Hydroxy silicone oil was added according to the ratio, and the drop was finished within 2 h. When the temperature of the reaction system started to rise and the viscosity increased, heating was stopped and the stirring rate was increased. The reaction continued at 70 °C after the drop. The reaction was continued at 70 °C for 1 h and then reduced to room temperature and discharged. The reaction equation for the synthesis of the prepolymer is shown in Scheme 1.



Scheme 1. Reaction equation for the synthesis of PU-Si.

2.4. Determination of the Free-NCO Content

The titration method was followed as in reference [40]. Briefly, 1.0000 g of the sample in dry iodine was weighed in a measuring flask, 10 mL of acetone was added to dissolve the sample, 20.00 mL of butylamine-acetone solution was added accurately, the flask was closed, shaken thoroughly, and left for 15 min; subsequently, 3 drops of bromocresol green indicator was added and titration was performed with 0.1000 mol/L HCl standard solution to the endpoint (solution from blue to yellow). The content is calculated in Equation (1).

$$\omega = \frac{(V_0 - V_1) \times c \times 0.04202}{m} \times 100\% \quad (1)$$

where V_0 —Volume of standard dilute hydrochloric acid consumed in blank test, mL; V_1 —amount of dilute hydrochloric acid consumed by the sample, mL; c —molar concentration of standard dilute hydrochloric acid, mol/L; m —the mass of the sample, g.

2.5. Production Processes for Insulating Coatings

The production processes were followed as in reference [41]. Briefly, polydimethylsiloxane (PDMS), prepolymer (PU-Si), SiO₂, CaCO₃, and Mg(OH)₂ were added to the reactor and stirred at 120 °C for 1 h. The material was mixed well and then stirred under a vacuum for 3 h. After natural cooling, the temperature was reduced to 50–70 °C, and the

silicone oil was added, the temperature was maintained, and the mixing was continued for 1 h. Finally, dimethyl silicone oil, MOS, KH792, and dibutyltin laurate were added, continue stirring for 3 h, and encapsulated. The sample formulations are shown in Table 1.

Table 1. Sample formulations.

Entry	PDMS (g)	PU-Si (g)	SiO ₂ (g)	CaCO ₃ (g)	Dimethyl Silicone Oil (g)	MOS (g)	KH792 (g)	Dibutyltin Laurate (g)	Mg(OH) ₂ (g)
1	100	0	10	90	10	5	5	0.3	10
2	90	10	10	90	10	5	5	0.3	10
3	80	20	10	90	10	5	5	0.3	10
4	70	30	10	90	10	5	5	0.3	10
5	60	40	10	90	10	5	5	0.3	10
6	50	50	10	90	10	5	5	0.3	10
7	70	30	5	95	10	5	5	0.3	10
8	70	30	15	85	10	5	5	0.3	10
9	70	30	10	90	10	6	5	0.3	10
10	70	30	10	90	10	7	5	0.3	10
11	70	30	10	90	10	8	5	0.3	10
12	70	30	10	90	10	9	5	0.3	10
13	70	30	10	90	10	10	5	0.3	10
14	70	30	10	90	10	7	1	0.3	10
15	70	30	10	90	10	7	3	0.3	10
16	70	30	10	90	10	7	7	0.3	10
17	70	30	10	90	10	7	9	0.3	10
18	70	30	10	90	10	7	5	0.1	10
19	70	30	10	90	10	7	5	0.2	10
20	70	30	10	90	10	7	5	0.4	10
21	70	30	10	90	10	7	5	0.3	0
22	70	30	10	90	10	7	5	0.3	20
23	70	30	10	90	10	7	5	0.3	30
24	70	30	10	90	10	7	5	0.3	40

3. Results

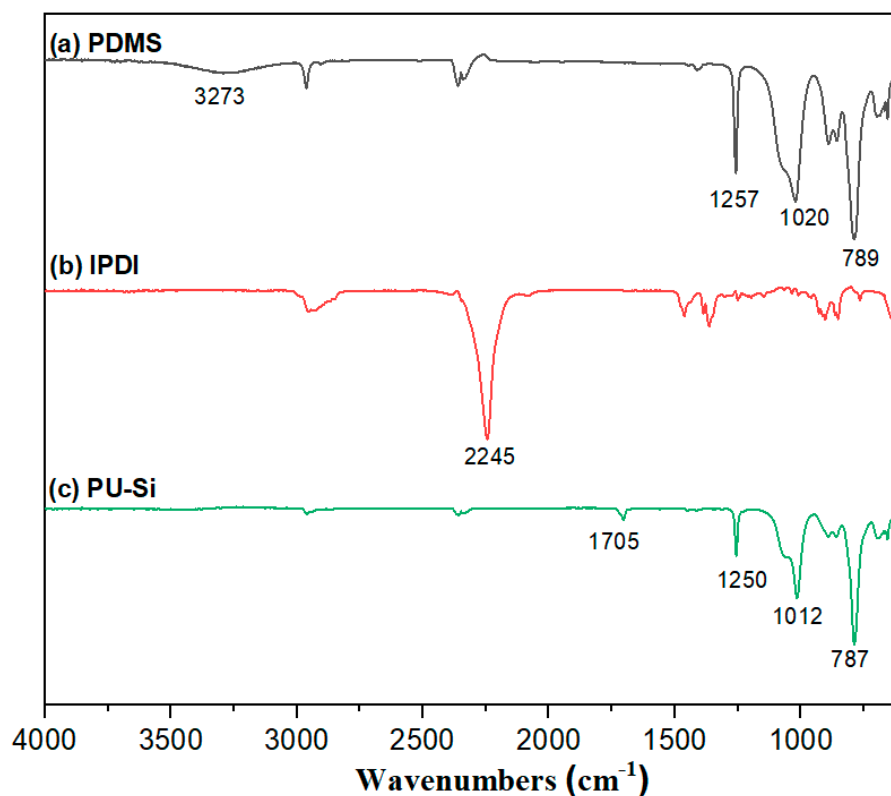
3.1. Optimal Synthesis Process for Prepolymer

PDMS has high hardness and poor elasticity after vulcanization when its viscosity is too low, and poor extrusion and processing properties when its viscosity is too high. Therefore, PDMS with a viscosity of 35 cst was chosen as the raw material for the experiments, and the optimum synthesis of the prepolymer was studied, as shown in Table 2. First, we fixed the reaction temperature (70 °C) and reaction time (3 h) and investigated the effect of the PDMS/IPDI molar ratio on the reaction. It is apparent that the reaction gradually reacted completely, as the PDMS/IPDI molar ratio increased, and the remaining NCO content gradually decreased to below 2%. When the PDMS/IPDI molar ratio was 2.5:1, the reaction was complete (the remaining NCO content was up to 1.7%). The effect of temperature on the reaction was then investigated by fixing the PDMS/IPDI molar ratio at 2.5:1. The temperature 60 °C was low, and the reaction was slightly slower. Moreover, 80–90 °C was the same as 70 °C, but the free NCO in the system was prone to side reactions when heated at high temperatures for a long time; therefore, 70 °C was chosen as the reaction temperature. Finally, the effect of reaction time on the reaction was investigated. Although the reaction will proceed more completely by extending the reaction time, there will be an occurrence of side reactions for a long reaction time; therefore, a reaction time of 3 h was chosen. The reaction conditions for the silicone to polyurethane prepolymer were set at a PDMS/IPDI molar ratio of 2.5:1, a reaction temperature of 70 °C, and a reaction time of 3 h.

Table 2. Optimization of reaction conditions.

Entry	Molar Ratio of PDMS/IPDI	Reaction Temperature (°C)	Reaction Time (h)	Content of Residual NCO in the Product (%)
1	2:1	70	3	6.5
2	2.3:1	70	3	2.1
3	2.5:1	70	3	1.7
4	3:1	70	3	1.1
5	4:1	70	3	1.0
6	2.5:1	60	3	5.6
7	2.5:1	80	3	1.8
8	2.5:1	90	3	1.6
9	2.5:1	70	2	4.6
10	2.5:1	70	4	1.0

The Infrared spectroscopy (IR) were able to verify the structure of the prepolymer [42–44]. As shown in Figure 1a, 3273 cm^{-1} was the characteristic absorption peak of the hydroxyl groups in PDMS, 1020 cm^{-1} was the stretching vibration absorption of Si–O–Si, 1257 cm^{-1} was the symmetric bending absorption peak of the methyl group in Si–CH₃, and 789 cm^{-1} was the stretching vibration absorption peak of Si–C. As shown in Figure 1b, IPDI shows a characteristic absorption peak of –NCO at 2245 cm^{-1} . In the IR spectra of the prepolymer (Figure 1c), a new C=O(–NHCOO–) stretching vibration absorption peak at 1705 cm^{-1} , a Si–O–Si stretching vibration absorption peak at 1012 cm^{-1} , a Si–C symmetric bending absorption peak at 1250 cm^{-1} , and a Si–C stretching vibration peak at 787 cm^{-1} are apparent. Meanwhile, the absorption peak of active hydrogen at 3273 cm^{-1} became weaker, and the characteristic absorption peak of –NCO at 2245 cm^{-1} disappeared. These data indicate that PDMS completely reacted with IPDI, and the polyurethane was successfully embedded in the molecular chain of PDMS.

**Figure 1.** Infrared spectra of IPDI, PDMS, and PU-Si.

3.2. Mechanical Properties of Samples

The effects of different ratios of PDMS and PU-Si on the tensile strength and elongation at break were investigated, and the specific data are shown in Table S1 and Figure 2. When only PDMS was added, the tensile strength and elongation at the break of sample 1 were 0.83 MPa and 107%, respectively (Entry 1, Figure S1). The introduction of polyurethane as a hard segment into the silicone rubber material was effective in improving the mechanical properties of the silicone. Compared to sample 1, other samples with the addition of the prepolymer PU-Si showed some improvement in the tensile strength and elongation at the break of the film (Entry 2–6). Sample 2 showed a 165% increase in tensile strength and a 119% growth rate elongation at the break compared to sample 1. The other samples (3–6) showed an increase in tensile strength between 244% and 318% and a growth rate elongation at the break between 88% and 146% compared to sample 1 (Figure S2). This should probably be attributed to the fact that the addition of PU improved the degree of microphase separation of the silicone rubber material [45]. However, when the amount of PU-Si was further increased, the tensile strength of the adhesive film gradually decreased, probably due to the incompatibility between PDMS and polyurethane, resulting in a further narrowing of the interface between the soft and hard segments [46]. The tensile strengths of the PU-Si prepolymerised samples were all above 2 MPa, and all had good mechanical properties as wrapping materials.

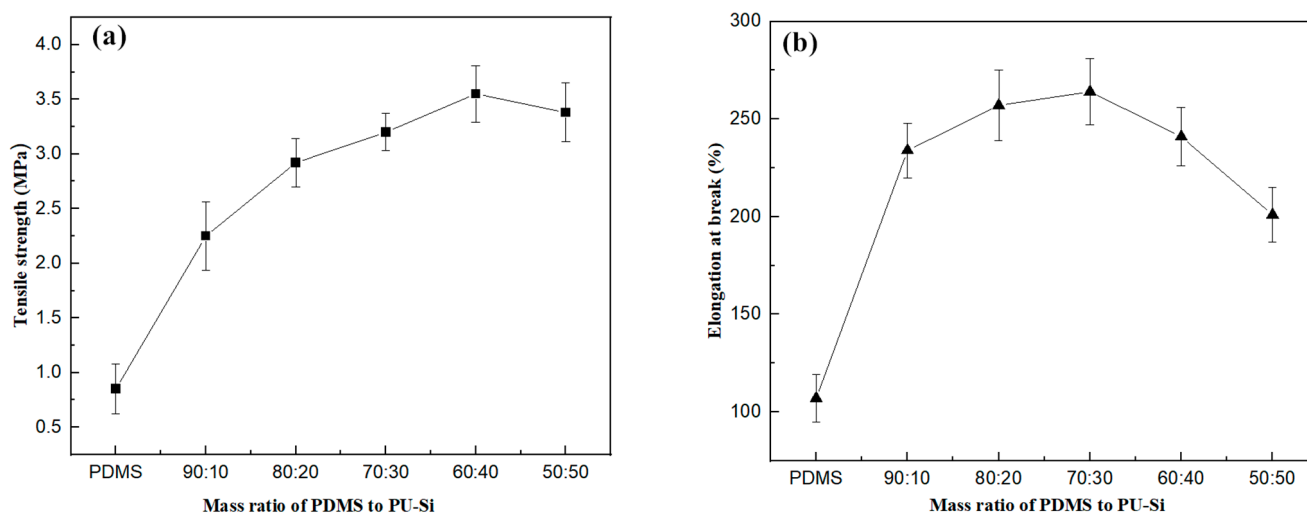


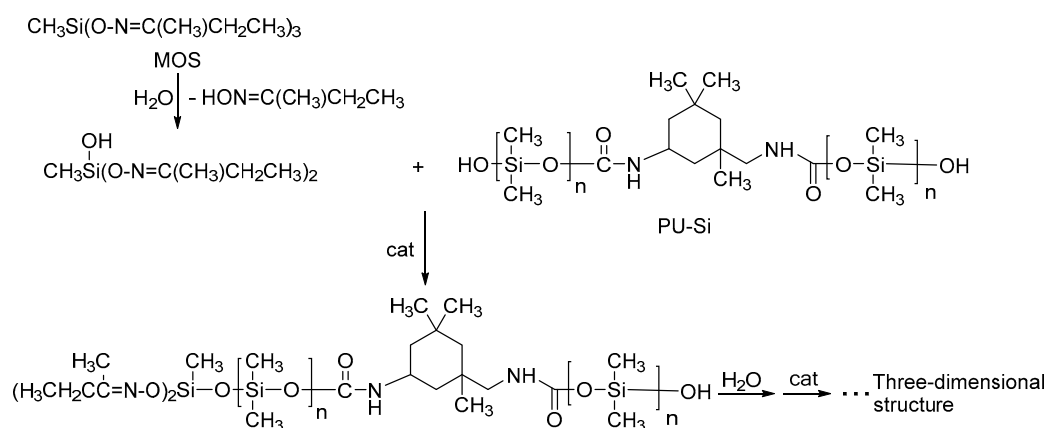
Figure 2. Effect of mass ratio of PDMS to IPDI on mechanical properties of samples. (a) Tensile strength of samples; (b) Elongation at the break of samples.

Different fillers have different effects on the performance of silicone rubber. SiO_2 contains -OH, which can produce strong interactions (hydrogen bonding) with the molecular chains of silicone rubber. Compared with SiO_2 , CaCO_3 is cheaper and easier to disperse evenly in rubber. Both SiO_2 and CaCO_3 can improve the hardness of vulcanized rubber and have strong reinforcing properties. The addition of SiO_2 and CaCO_3 to vulcanized rubber as reinforcing materials can lead to a significant improvement in the mechanical properties of rubber (Table 1, entries 1–8). However, with the addition of more SiO_2 , the dynamic viscosity of the rubber becomes higher, and the extrusion performance decreases, which is not favorable for insulating coating extrusion. Therefore, according to the field experiment, we chose to add $\text{SiO}_2:\text{CaCO}_3 = 10:90$ as the suitable ratio for the sample formulation.

3.3. Effect of the Amount of Crosslinker on the Surface Drying Time and Deep Curing Performance of the Coating

Crosslinkers are a key component of room-temperature vulcanized rubbers. Deke-toxime silicone rubber has the advantages of good adhesion, non-corrosive, storage stability, and fast surface and internal curing of the rubber layer, and is widely used in the field

of insulation of electrical equipment. The crosslinking agent used in this experiment was methyl tris-butanone oxime silane. The crosslinking and curing process is shown in Scheme 2. First, the crosslinking agent was subjected to the atmospheric moisture reaction to remove the ketoxime group in order to generate silanol, followed by the -OH group in the silanol and the -OH in the PU-Si or PDMS condensation reaction. Through repeated de-ketoxime processes and condensation, the silicone rubber crosslinking curing formed a three-dimensional network structure.



Scheme 2. Curing process of room-temperature vulcanized rubber.

As Table S2 and Figure 3 show, the higher the amount of crosslinker, the shorter the drying time of the silicone rubber. This is because increasing the crosslinking agent increases the chance of the crosslinking agent combining with water vapor. When the amount of crosslinker exceeds 8 g, the effect of increasing the crosslinker on the drying time becomes less and less. With the increase of the crosslinking agent content, the deep curing rate of vulcanized rubber shows a trend of first increasing and then decreasing. In the case of a moderate increase in the crosslinking agent, the chance of the intermolecular condensation of the crosslinking agent occurring correspondingly increases, with a positive effect on deep curing. With the further excess of the crosslinking agent content, the increase of the crosslinking density has a barrier effect on water vapor, such that the moisture does not easily diffuse into the interior of the rubber, resulting in slowing down the vulcanization speed. Therefore, according to the experimental results, we chose the amount of crosslinking agent to be 7 g.

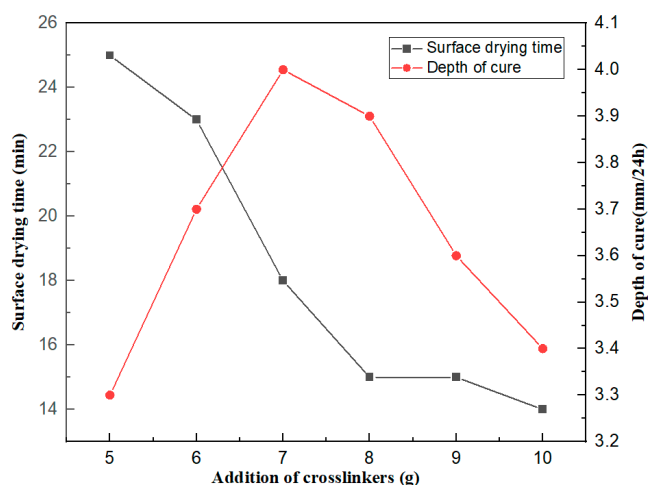


Figure 3. Effect of the amount of crosslinker on the surface drying time and deep curing performance of the coating.

3.4. Effect of Coupling Agent KH792 on Interfacial Bonding Properties

The silane coupling agent is a class of silicone compound containing two different chemical functional groups in the molecule, which improves the adhesive performance of the material surface by improving the wettability of the adhesive and fully bonding with the bonded material. In this paper, the amine coupling agent KH792 was chosen as a tackifier. The experimental results are detailed in Figure 4 and Table S3. When KH792 was added at the amount of 1–9 g, the obtained silicone rubber had good adhesion to the experimental substrates. When the amount of coupling agent exceeded a certain limit, it did not contribute to the bonding performance of the substrate. The adhesion properties did not continue to improve with the addition of the coupling agent, probably because the coupling agent molecules migrated to the bonding interface and formed only a single molecular deposit layer on the surface. The best adhesion was obtained at the additional amount of 5 g (Figure S3).

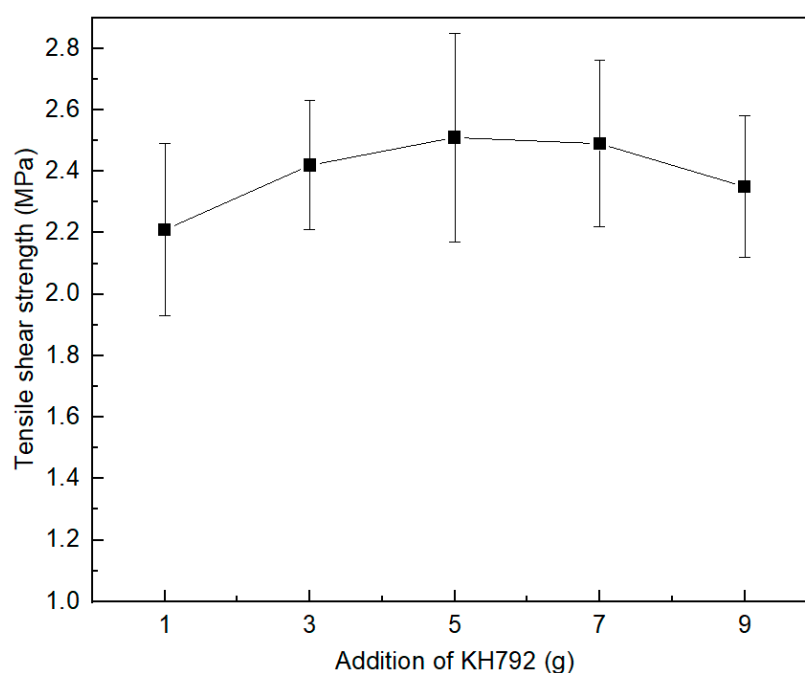


Figure 4. Effect of coupling agent KH792 on interfacial bonding properties.

3.5. Effect of Catalyst on Surface Drying Time of the Coating

The amount of catalyst also affects the surface drying time. As Table S2 shows, the surface drying time of the coating was reduced with the increase in the amount of catalyst; when the amount of catalyst was 0.1 g, the surface drying time was 31.3 min, and when the amount of catalyst was increased to 0.4 g, the surface drying time was reduced to 13.9 min. Compared to the silicone rubber with 0.3 g of catalyst, the tear strength of the silicone rubber with 0.4 g of catalyst started to decrease (Table S3). The decrease in mechanical properties may be because the growth of the molecular chains was affected due to too rapid vulcanization. Therefore, a catalyst dosage of 0.3 g was chosen for this experiment.

3.6. Influence of the Amount of Flame Retardant Filler on the Flame Retardant Properties of Silicone Rubber

Although silicone rubber itself has high temperature resistance and flame retardant self-extinguishing properties, without the addition of flame retardant material, silicone rubber has difficulty meeting the requirements of high-voltage power transmission lines. Magnesium hydroxide has good flame retardant properties and smoke dissipation properties and promotes the role of carbon formation, as a non-halogen flame retardant can effectively improve the heat and flame retardant properties of cable materials [47–49]. Ta-

ble 3 shows the vertical burning time of sealants with different amounts of flame retardant fillers. It can be seen that the flame retardancy of silicone rubber improved significantly with the increase addition of $Mg(OH)_2$. With the addition of 10 g of $Mg(OH)_2$, the silicone rubber was already flame retardant, and the flame retardant performance could reach FV-2; with the addition of 20 g of $Mg(OH)_2$, the silicone rubber was already flame retardant, and the flame retardant performance could reach FV-1; and with the addition of 40 g of $Mg(OH)_2$, the flame retardant performance of the silicone rubber could reach FV-0 level. With the increase in the amount of magnesium hydroxide, the flame retardant performance gradually increased. This may be due to the decomposition of magnesium hydroxide in absorbing heat from the surface of the combustible material, releasing a large amount of water to dilute the oxygen on the surface of the combustible material, and the decomposition of the generated active magnesium oxide attached to the surface of the combustible material and further prevented the combustion.

Table 3. Effect of the amount of $Mg(OH)_2$ on the flame retardant properties of silicone rubber.

Entry	10 (10 g)	21 (0 g)	22 (20 g)	23 (30 g)	24 (40 g)
Sample extinction time (s)	53	>60	45	31	17
tensile strength (MPa)	3.37 ± 0.31	3.45 ± 0.24	3.31 ± 0.28	3.23 ± 0.26	3.14 ± 0.27
elongation at break (%)	259 ± 22	268 ± 14	251 ± 19	238 ± 33	223 ± 21
Volumetric resistivity (Ω -cm)	7.15×10^{14}	9.88×10^{14}	5.55×10^{14}	4.36×10^{14}	2.06×10^{14}
Breakdown voltage (kV/mm)	22.3	23.5	22.1	21.7	20.2

To select the optimum conditions for the addition of the flame retardant, further thermal weight loss analysis and surface morphology analysis were carried out on the samples.

3.6.1. Thermogravimetric Analyses

Figure 5 and S4 show the thermal weight loss graphs of silicone rubber samples 10, 21, 23, and 24. The decomposition interval of silicone rubber was divided into two intervals: the first one (400–500 °C) is for small and medium molecules of silicone rubber, and the second one (500–700 °C) is for large molecules and powders.

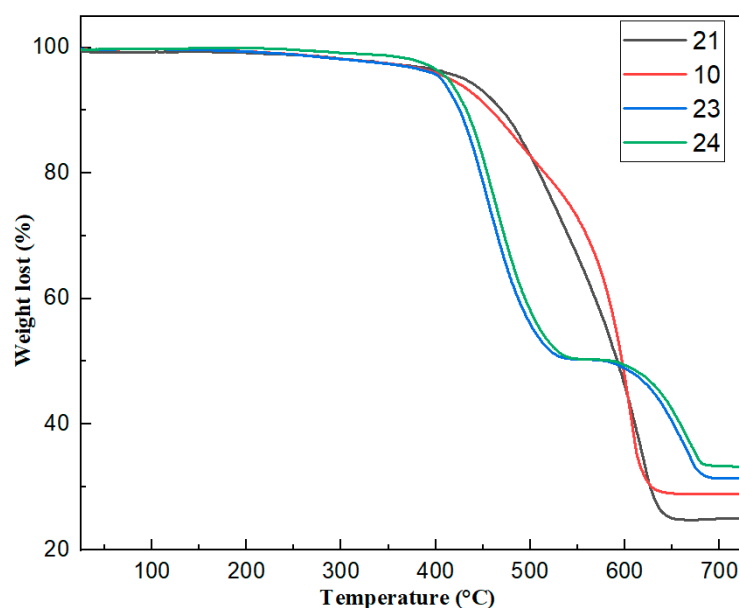


Figure 5. TG curves of different silicone rubbers: 21 (0 g $Mg(OH)_2$), 10 (10 g $Mg(OH)_2$), 23 (30 g $Mg(OH)_2$), 24 (40 g $Mg(OH)_2$).

Silicone rubber (10), without the addition of magnesium hydroxide, started to lose weight at 415 °C and ended at 630 °C, with a residual mass of 29.79% for the silicone rubber coating (Figure 5). The thermal weight loss curves of all the samples in the first warming interval were similar: all started to show a mass loss at around 400 °C. The thermogravimetric curves of the composites with a small amount of magnesium hydroxide (21, 10 g) added did not change much compared to the silicone rubber (10) without the addition of flame retardant material. When more than 20 g of magnesium hydroxide (23, 30 g) was added, the samples first showed a strong thermal weight loss at 390–500 °C. This may be due to the decomposition of magnesium hydroxide at 390 °C, producing water vapor and high-temperature-resistant solid magnesium oxide. This interval overlaps with the first decomposition interval of silicone rubber, which should precede the decomposition reaction of rubber during the heating process and absorb a lot of heat during the decomposition, which can make the initial decomposition of silicone rubber be effectively curbed. From Figure 5, we can see that adding more than 30 g of magnesium hydroxide significantly improved the thermal stability of silicone rubber material.

3.6.2. SEM Analysis

Table 3 shows that both the tensile strength and elongation at the break of the silicone rubber decreased with increasing magnesium hydroxide. The changes in mechanical properties of the four samples can also be verified in the scanning electron micrographs. Figure 6 shows that the surface of the four sample films became more and more uneven with the increase of magnesium hydroxide content; the particles were dispersed more and more unevenly, and some of the particles in the films showed agglomeration. The composition of sample 23 was examined by Energy dispersive spectrum (EDS). Table S4 and Figure 7 show the atomic percentages of the Si, N, Mg, O, and C elements, with higher content of Si and O atoms and 7.17% of Mg atoms. The results of the flame retardation experiments and thermogravimetric analysis tests showed that the added $Mg(OH)_2$ improved the fire performance of the insulating coating.

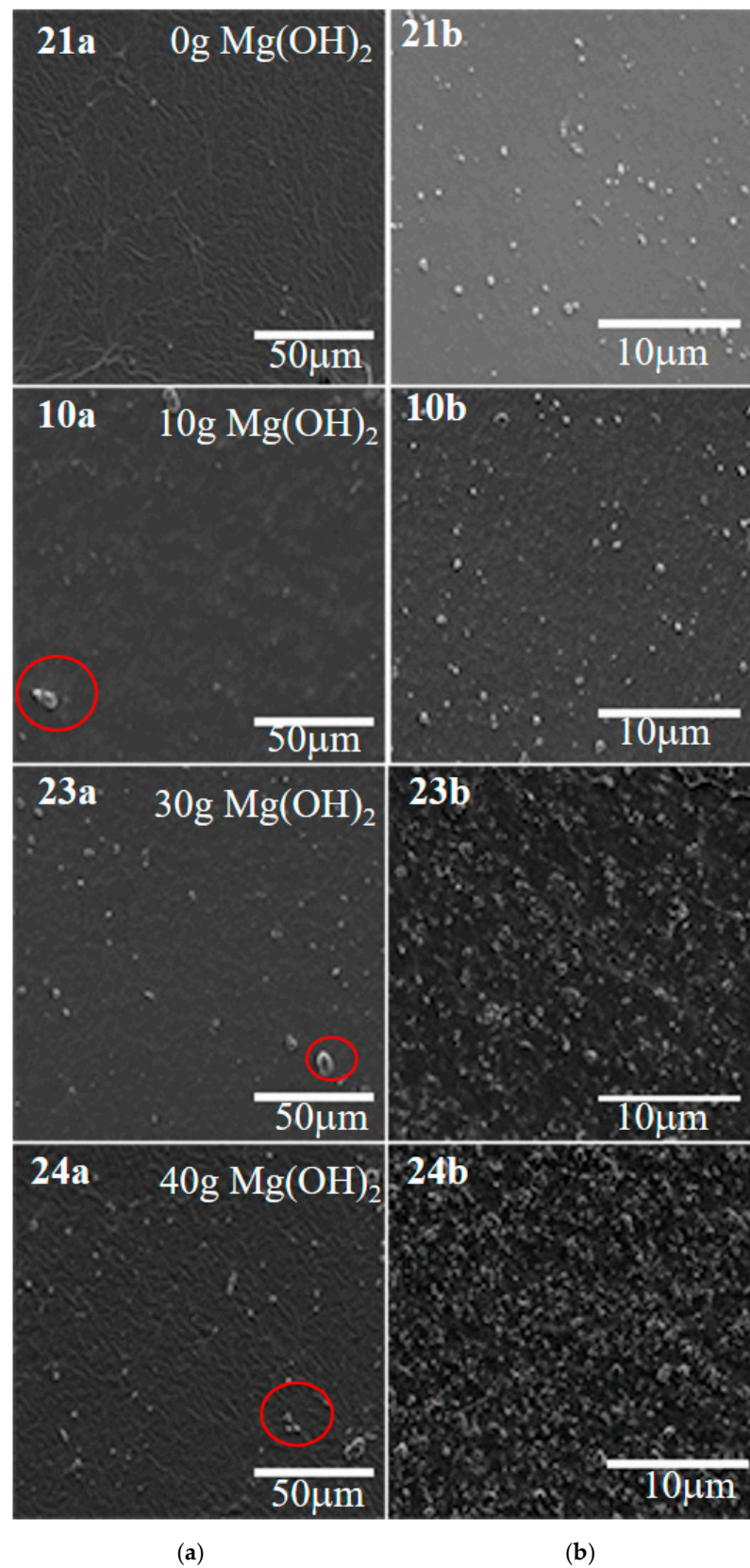


Figure 6. SEM images of four different samples: (a) planar scans, (b) fracture surface scan. Red circles represent uneven particle dispersion.

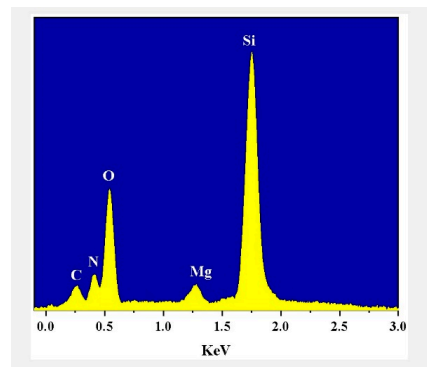


Figure 7. EDS Analysis of sample 23.

3.6.3. Electrical Properties Testing of Silicone Rubber

As Table 3 shows, the volume resistivity of silicone rubber decreased continuously with increasing $\text{Mg}(\text{OH})_2$. When the nano addition was below 20 g, the volume resistivity of the rubber changed less. When the amount of $\text{Mg}(\text{OH})_2$ was increased by 40 g, the volume resistivity of the silicone rubber changed to 2.06×10^{14} . The breakdown voltage of the silicone rubber with $\text{Mg}(\text{OH})_2$ was above 20 kV/mm, which meets the laying of the 10 kV overhead cable. The final choice was adding 30 g of magnesium hydroxide as the addition of flame retardants.

3.7. Field Trials and Applications

As shown in Figure 8a, the room-temperature vulcanized rubber coating with the coating robot independently developed by the State Grid Hubei Electric Power Company Xiaogan Power Supply Company was simulated in the laboratory. As shown in Figure 8b, the completed wrapped rubber coating could stick closely to the cable, and no air bubbles were generated during the coating process, while the coating did not drip hang. The product after the experiment was tested by a third-party testing company, and its properties, such as flame retardant and electrical insulation, meet the requirements for wrapping 10 kV cables. The coating has now been applied to the 10 kV cable line renovation of the State Grid Hubei Electric Power Co. Ltd. (Figure 8d).

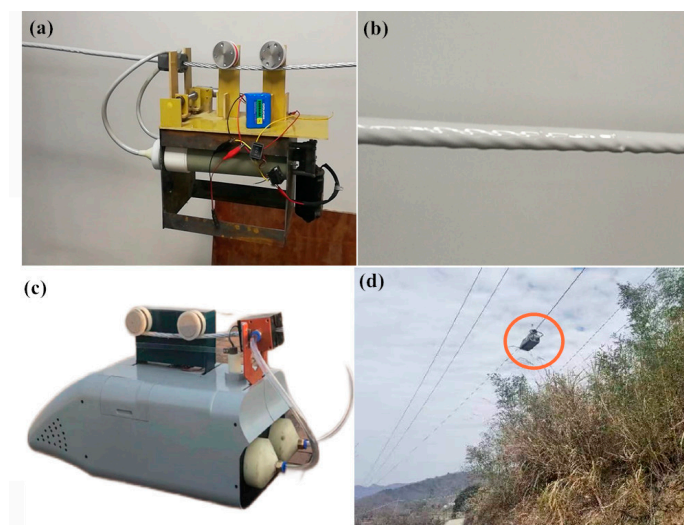


Figure 8. Field trials and applications: (a) Room temperature vulcanized rubber coating with insulation coating robot (testing machine) on steel cable for coating experiments. (b) Room-temperature vulcanized rubber coating completes the cladding. (c) Insulation coating robot. (d) Field working diagram of room-temperature vulcanized rubber coating with insulation coating robot completing wrapping on 10 kV cable. (The red circle represents an insulated coating robot at work.)

4. Conclusions

The silicone–polyurethane prepolymer was obtained by modifying α,ω -dihydroxy polydimethylsiloxane with isophorone diisocyanate. Then, the prepolymer was mixed with PDMS, MOS, SiO₂, and Mg(OH)₂ to prepare an insulating coating with a short surface drying time, fast curing speed, good mechanical properties, and excellent insulation performance. Its volume resistivity is more than $4 \times 10^{14} \Omega \cdot \text{cm}$, the breakdown voltage is more than 20 kV/mm, and the flame retardant performance is up to the FV-1 level. The coating preparation method is simple, has good controllability, is suitable for mass production, and can be used for the transformation of 10 kV overhead wires, with significant economic and social benefits.

Supplementary Materials: The following supporting information can be downloaded at: <https://www.mdpi.com/article/10.3390/coatings13050837/s1>, Figure S1: Image of the test sample 10; Figure S2: Tensile-elongation curve for different mass ratios (Samples of 1–6); Figure S3: Shear strength-displacement curve of rubber with 5 g of KH792; Figure S4. Shapes of samples 10, 21, 23, and 24; Table S1: Mechanical properties of different ratios of PDMS and PU-Si; Table S2: Effect of different amounts of crosslinker on surface drying time and depth of cure; Table S3: Effect of coupling agent KH792 on interfacial bonding properties; Table S4: Content of elements in sample 23.

Author Contributions: Designed the experiment, W.L.; experiments and writing—draft manuscript, W.W.; review and editing, A.L. and C.Q.; data curation, F.Y.; writing—review and editing, P.Z., Z.L., F.L., J.J. and J.Z. All authors have read and agreed to the published version of the manuscript.

Funding: This research was funded by the Xiaogan City Natural Science Program of China (Grant No.: XGKJ2022010085).

Institutional Review Board Statement: Not applicable.

Informed Consent Statement: Not applicable.

Data Availability Statement: Supporting data are available from the corresponding authors.

Conflicts of Interest: The authors declare no conflict of interest.

References

1. Péter, Z.; Farzaneh, M.; Kiss, L.I. Assessment of the current intensity for preventing ice accretion on overhead conductors. *IEEE Trans. Power Deliv.* **2006**, *22*, 565–574. [[CrossRef](#)]
2. Cimini, C.A., Jr.; Fonseca, B.Q.A. Temperature profile of progressive damaged overhead electrical conductors. *Int. J. Electr. Power Energy Syst.* **2013**, *49*, 280–286. [[CrossRef](#)]
3. Qu, N.; Li, Z.; Zuo, J.; Chen, J. Fault detection on insulated overhead conductors based on DWT-LSTM and partial discharge. *IEEE Access* **2020**, *8*, 87060–87070. [[CrossRef](#)]
4. Rao, C.; Song, Y.; Wang, H.; Wang, J.; Jing, F. Robotic Visual Inspection and Positioning Method for Flexible Wire Coating Operation. In Proceedings of the 2022 12th International Conference on CYBER Technology in Automation, Control, and Intelligent Systems (CYBER), Changbai Mountain, China, 27–31 July 2022; IEEE: Piscataway, NJ, USA; pp. 247–252.
5. Yan, Y.; Xu, X.; Xiao, Z.; Tong, X. Mechanism design of electric robot of distribution network for cut off or connection of leading wire. In *IOP Conference Series: Earth and Environmental Science*; IOP Publishing: Bristol, UK, 2019; Volume 237, p. 062027.
6. Zhou, F.; Zhu, J.; An, N.; Wang, C.; Liu, J.; Long, L. The anti-icing and deicing robot system for electricity transmission line based on external excitation resonant. *IEEE Trans. Electr. Electron. Eng.* **2020**, *15*, 593–600. [[CrossRef](#)]
7. Catterson, V.; Castellon, J.; Pilgrim, J.; Saha, T.K.; Ma, H.; Vakilian, M.; Moradnouri, A.; Gholami, M.; Sparling, B. The impact of smart grid technology on dielectrics and electrical insulation. *IEEE Trans. Dielectr. Electr. Insul.* **2015**, *22*, 3505–3512. [[CrossRef](#)]
8. Wang, Z.-S.; Yanagida, M.; Sayama, K.; Sugihara, H. Electronic-insulating coating of CaCO₃ on TiO₂ electrode in dye-sensitized solar cells: Improvement of electron lifetime and efficiency. *Chem. Mater.* **2006**, *18*, 2912–2916. [[CrossRef](#)]
9. Li, Y.; Sheng, L.; Wu, J.; Li, X.; Zhao, J.; Zhang, M.; Yuan, Y.; Peng, B. Influence of insulating coating on aluminum wire explosions. *Phys. Plasmas* **2014**, *21*, 102513. [[CrossRef](#)]
10. Liu, S.; Veysey, S.W.; Fifield, L.S.; Bowler, N. Quantitative analysis of changes in antioxidant in crosslinked polyethylene (XLPE) cable insulation material exposed to heat and gamma radiation. *Polym. Degrad. Stab.* **2018**, *156*, 252–258. [[CrossRef](#)]
11. Green, C.; Vaughan, A.; Stevens, G.; Pye, A.; Sutton, S.; Geussens, T.; Fairhurst, M. Thermoplastic cable insulation comprising a blend of isotactic polypropylene and a propylene-ethylene copolymer. *IEEE Trans. Dielectr. Electr. Insul.* **2015**, *22*, 639–648. [[CrossRef](#)]

12. Jia, Z.; Fang, S.; Gao, H.; Guan, Z.; Wang, L.; Xu, Z. Development of RTV silicone coatings in China: Overview and bibliography. *IEEE Electr. Insul. Mag.* **2008**, *24*, 28–41.
13. Zhang, Z.; Qiao, X.; Xiang, Y.; Jiang, X. Comparison of surface pollution flashover characteristics of RTV (room temperature vulcanizing) coated insulators under different coating damage modes. *IEEE Access* **2019**, *7*, 40904–40912. [[CrossRef](#)]
14. Li, Z.; Yin, F.; Cao, B.; Wang, L.; Shao, S.; Farzaneh, M. Pollution flashover performance of RTV coatings with partial damage. *Int. J. Electr. Power Energy Syst.* **2020**, *121*, 106102. [[CrossRef](#)]
15. Taghvaei, M.; Sedighzadeh, M.; NayebPashae, N.; Fini, A.S. Thermal stability of nano RTV vs. RTV coatings in porcelain insulators. *Therm. Sci. Eng. Prog.* **2020**, *20*, 100696. [[CrossRef](#)]
16. Gao, W.; Zhang, J.; Wei, M.; Wan, D.; Wang, Y.; Du, Y. The Improvement in Electrical Properties of RTV Silicone Rubber by the Introduction of TiO₂ rNanocomposite. In Proceedings of the 2022 IEEE Conference on Electrical Insulation and Dielectric Phenomena (CEIDP), Denver, CO, USA, 30 October–2 November 2022; pp. 293–296.
17. Zhi, M.; Yang, X.; Fan, R.; Yue, S.; Zheng, L.; Liu, Q.; He, Y. A comprehensive review of reactive flame-retardant epoxy resin: Fundamentals, recent developments, and perspectives. *Polym. Degrad. Stab.* **2022**, *201*, 109976. [[CrossRef](#)]
18. Han, Q.; Sheng, Y.; Liu, X.; Zhang, X.; Chen, X.; Li, B.; Han, Z. Carbon fiber reinforced epoxy composite combining superior electrochemical energy storage and mechanical performance. *Chem. Eng. J.* **2022**, *437*, 135228. [[CrossRef](#)]
19. Liu, Z.; Xu, J.; Zhu, X.; Liu, F.; Fang, Z. Study on discharge characteristics and improving surface hydrophobicity of epoxy resin by nanosecond pulse excited argon/hexamethyldisiloxane jet array. *High Volt.* **2022**, *7*, 771–781. [[CrossRef](#)]
20. Chattopadhyay, D.K.; Raju, K. Structural engineering of polyurethane coatings for high performance applications. *Prog. Polym. Sci.* **2007**, *32*, 352–418. [[CrossRef](#)]
21. Hepburn, C. *Polyurethane Elastomers*; Springer Science & Business Media: Berlin, Germany, 2012.
22. Akindoyo, J.O.; Beg, M.; Ghazali, S.; Islam, M.; Jeyaratnam, N.; Yuvaraj, A. Polyurethane types, synthesis and applications—a review. *Rsc Adv.* **2016**, *6*, 114453–114482. [[CrossRef](#)]
23. Ronca, S. Polyethylene. In *Brydson's Plastics Materials*; Elsevier: Amsterdam, The Netherlands, 2017; pp. 247–278.
24. Ouyang, Y.; Mauri, M.; Pourrahimi, A.M.; Östergren, I.; Lund, A.; Gkourmpis, T.; Prieto, O.; Xu, X.; Hagstrand, P.-O.; Müller, C. Recyclable polyethylene insulation via reactive compounding with a maleic anhydride-grafted polypropylene. *ACS Appl. Polym. Mater.* **2020**, *2*, 2389–2396. [[CrossRef](#)]
25. Ding, M.; He, W.; Wang, J.; Wang, J. Performance Evaluation of Cross-Linked Polyethylene Insulation of Operating 110 kV Power Cables. *Polymers* **2022**, *14*, 2282. [[CrossRef](#)]
26. Gill, Y.Q.; Ehsan, H.; Mehmood, U.; Irfan, M.S.; Saeed, F. A novel two-step melt blending method to prepare nano-silicized-silica reinforced crosslinked polyethylene (XLPE) nanocomposites. *Polym. Bull.* **2022**, *79*, 10077–10093. [[CrossRef](#)]
27. Stelescu, M.D.; Sonmez, M.; Georgescu, M.; Alexandrescu, L.; Nituica, M.; Gurau, D. Polymeric compounds based on thermoplastic elastomer styrene-butadiene-styrene block copolymers and silicic rubber powder. *Prog. Rubber Plast. Recycl. Technol.* **2022**, *38*, 311–327. [[CrossRef](#)]
28. Mokhtari Aghdami, R.; Mousavi, S.R.; Estaji, S.; Dermeni, R.K.; Khonakdar, H.A.; Shakeri, A. Evaluating the mechanical, thermal, and antibacterial properties of poly (lactic acid)/silicone rubber blends reinforced with (3-aminopropyl) triethoxysilane-functionalized titanium dioxide nanoparticles. *Polym. Compos.* **2022**, *43*, 4165–4178. [[CrossRef](#)]
29. Alikhani, E.; Mohammadi, M.; Sabzi, M. Preparation and study of mechanical and thermal properties of silicone rubber/poly (styrene-ethylene butylene-styrene) triblock copolymer blends. *Polym. Bull.* **2022**, *1–22*. [[CrossRef](#)]
30. da Silva, C.R.; Masini, J.C. Ethylene vinyl acetate copolymer is an efficient and alternative passive sampler of hydrophobic organic contaminants. A comparison with silicone rubber. *Environ. Pollut.* **2023**, *323*, 121258. [[CrossRef](#)]
31. Abd-Elhady, A.M.; Sleet, A.Y.; Izzularab, M.A.; Ibrahim, M.E. Polystyrene/silicone rubber blends with improved dielectric properties. *Electr. Eng.* **2023**, *1–13*. [[CrossRef](#)]
32. Maity, M.; Khatua, B.; Das, C. Polyblend systems of polyurethane rubber and silicone rubber in the presence of silane grafting agent. *J. Elastomers Plast.* **2001**, *33*, 211–224. [[CrossRef](#)]
33. Cui, Y.; Yan, T.; Pan, H.; Sun, H.; Bai, X.; Cao, L.; Zong, C. Preparation and Characterization of Intrinsically Compatibilized Thermoplastic Polyurethane and Silicone Rubber. *Macromol. Chem. Phys.* **2022**, *223*, 2100420. [[CrossRef](#)]
34. Zhang, H.-F.; Hao, Q.; Tian, H.-C.; Yao, P.-J.; Liu, X.-Y.; Yu, B.; Ning, N.-Y.; Tian, M.; Zhang, L.-Q. Polyurethane-polysiloxane Copolymer Compatibilized SiR/TPU TPV with Comfortable Human Touch Toward Wearable Devices. *Chin. J. Polym. Sci.* **2023**, *41*, 258–266. [[CrossRef](#)]
35. Chen, H.; Zheng, K.; Zhu, A.; Meng, Z.; Li, W.; Qin, C. Preparation of Bentonite/Chitosan Composite for Bleaching of Deteriorating Transformer Oil. *Polymers* **2020**, *12*, 60. [[CrossRef](#)]
36. Zheng, K.; Meng, Z.; Li, J.; Peng, S.; Huang, C.; Wang, W.; Li, W.; Qin, C. The Preparation and Characterization of a Cyanide-Free Brush-Plating Solution for Application in the Electric Power Industry. *Coatings* **2022**, *12*, 194. [[CrossRef](#)]
37. Meng, Z.; Zheng, K.; Huang, C.; Li, W.; Qin, C. A New Type of Coating Brush Plating Solution and Its Application Performance. *Coatings* **2022**, *12*, 134. [[CrossRef](#)]
38. Shao, J.; Yu, C.; Bian, F.; Zeng, Y.; Zhang, F. Preparation and properties of hydrophilic rosin-based aromatic polyurethane microspheres. *ACS Omega* **2019**, *4*, 2493–2499. [[CrossRef](#)]
39. Christenson, E.M.; Dadsetan, M.; Anderson, J.M.; Hiltner, A. Biostability and macrophage-mediated foreign body reaction of silicone-modified polyurethanes. *J. Biomed. Mater. Res. Part A* **2005**, *74*, 141–155. [[CrossRef](#)]

40. Chen, Q.; Xu, Z.; Sun, Z.; Sun, Y.; Song, J.; Zhang, X.; Huan, S.; Bai, L.; Gu, J. Engineering liquid pMDI into water-processable powder: Manufacture and application as waterborne additive. *J. Clean. Prod.* **2022**, *372*, 133767. [[CrossRef](#)]
41. Yang, X.; Li, Q.; Li, Z.; Xu, X.; Liu, H.; Shang, S.; Song, Z. Preparation and characterization of room-temperature-vulcanized silicone rubber using acrylpimarinic acid-modified aminopropyltriethoxysilane as a cross-linking agent. *ACS Sustain. Chem. Eng.* **2019**, *7*, 4964–4974. [[CrossRef](#)]
42. Burel, F.; Feldman, A.; Bunel, C. Hydrogenated hydroxy-functionalized polyisoprene (H-HTPI) and isocyanurate of isophorone diisocyanates (I-IPDI): Reaction kinetics study using FTIR spectroscopy. *Polymer* **2005**, *46*, 15–25. [[CrossRef](#)]
43. Mata, A.; Fleischman, A.J.; Roy, S. Characterization of polydimethylsiloxane (PDMS) properties for biomedical micro/nanosystems. *Biomed. Microdevices* **2005**, *7*, 281–293. [[CrossRef](#)]
44. Sun, N.; Wang, Z.; Xu, Y.; Cong, J.; Li, J.; Bai, L.; Huo, P.; Li, Z.; Liu, Y. Synthesis of cellulose nanofiber/polysiloxane-polyurea composite materials with self-healing and reprocessing properties. *Int. J. Biol. Macromol.* **2023**, *227*, 203–213. [[CrossRef](#)]
45. Choi, T.; Weksler, J.; Padsalgikar, A.; Runt, J. Microstructural organization of polydimethylsiloxane soft segment polyurethanes derived from a single macrodiol. *Polymer* **2010**, *51*, 4375–4382. [[CrossRef](#)]
46. Speckhard, T.A.; Cooper, S.L. Ultimate tensile properties of segmented polyurethane elastomers: Factors leading to reduced properties for polyurethanes based on nonpolar soft segments. *Rubber Chem. Technol.* **1986**, *59*, 405–431. [[CrossRef](#)]
47. Huang, H.; Tian, M.; Liu, L.; Liang, W.; Zhang, L. Effect of particle size on flame retardancy of Mg(OH)₂-filled ethylene vinyl acetate copolymer composites. *J. Appl. Polym. Sci.* **2006**, *100*, 4461–4469. [[CrossRef](#)]
48. Brostow, W.; Lohse, S.; Lu, X.; Osmanson, A.T. Nano-Al(OH)₃ and Mg(OH)₂ as flame retardants for polypropylene used on wires and cables. *Emergent Mater.* **2019**, *2*, 23–34. [[CrossRef](#)]
49. Gui, H.; Zhang, X.; Dong, W.; Wang, Q.; Gao, J.; Song, Z.; Lai, J.; Liu, Y.; Huang, F.; Qiao, J. Flame retardant synergism of rubber and Mg(OH)₂ in EVA composites. *Polymer* **2007**, *48*, 2537–2541. [[CrossRef](#)]

Disclaimer/Publisher's Note: The statements, opinions and data contained in all publications are solely those of the individual author(s) and contributor(s) and not of MDPI and/or the editor(s). MDPI and/or the editor(s) disclaim responsibility for any injury to people or property resulting from any ideas, methods, instructions or products referred to in the content.